Spectrum of Engineering Sciences
ISSN (e) 3007-3138 (p) 3007-312X
Volume 4, Issue 4, 2026

THE EFFECT OF LITHIUM DOPING ON THE GROWN ZINC OXIDE NANOSTRUCTURE AT LOW TEMPERATURE, AND IT'S ANTIBACTERIAL PROPERTIES

Zaheer Hussain Abbasi[*1], Fozia Khatoon Soomro[2], Shams Parveen[3], Deedar Ali Jamro[4]

[*1]*Nanomaterials Laboratory, Institute of Physics, University of Sindh Jamshoro, Pakistan.*
[2]*Dr. MA Kazi Institute of Chemistry, University of Sindh Jamshoro, Pakistan.*
[3]*Nanomaterials Laboratory, Institute of Physics, University of Sindh Jamshoro, Pakistan.*
[4]*Department of Physics and Electronics Shah Abdul Latif University Khairpur, Sindh, Pakistan*

[1]zaheerhussain77@gmail.com, [2]foziasoomro@gmail.com, [3]shams_khokhar@outlook.com, [4]deedar.jamro@salu.edu.pk

DOI: https://doi.org/10.5281/zenodo.19878184

Keywords
Staphylococcus aureus, Escherichia colie, Li-ZnO, (Nano Particles), (Aquas Chemical Growth), X-ray diffraction (XRD), SEM characterization, photoluminescence (Pl), Broth dilution method.

Article History
Received: 04 March 2026
Accepted: 11 April 2026
Published: 29 April 2026

Corresponding Author: *
Zaheer Hussain Abbasi

Abstract

Scientists, chemists, and business community were drawn attention towards the Zinc Oxide because of its advantageous physical, chemical, and biological properties. It has many desirable properties, including a large energy gap (3.37 eV) at room temperature, a higher excitation energy value (60 meV), a higher index of refraction, and good piezoelectric capabilities. On the other hand, zinc oxide and zinc oxide nanoparticles have demonstrated remarkable resistance to a variety of bacterial species.

Because of all these characteristics, ZnO's turns into considered valuable substance of the future. As a result, this material can be used by scientists and engineers in everyday applications like solar cells, gas detectors, ultraviolet light-emitting diodes, diode-based lasers, and antimicrobial treatments.

Moreover, the incorporation of impurities into their crystal structure ZnO demonstrates that they are proficient in both positive and negative type of bacterial species. ZnO is mostly an N-type semi-metal in terms of its nature. The Zn and O_2 defects in structure are responsible for the N-type behavior. However, the occupation of holes by existing electrons makes it difficult to generate stable p-type zinc oxide.

The aqueous chemical growth approach was used in this study to create lithium-incorporated zinc oxide nanoparticles. It investigates their optical, structural, and antimicrobial properties against Escherichia coli and Staphylococcus aureus bacteria. Nano-scale crystal rods created by aqueous chemical growth have been studied using a variety of methods, including photoluminescence, scanning electron microscopy, and X-ray diffraction. In this sense, the antibacterial properties have been observed over two distinct bacterial strains, Escherichia coli and Staphylococcus aureus, using the Broth Dilution Method.

Furthermore, a study using X-ray diffraction has confirmed that the produced nanoparticles are wurtzite and hexagonal. Similarly, all of the produced nanostructures are rod-like, one-dimensional, and have the same dimensional

character, according to a study conducted using a scanning electron microscope. Ultimately, the photoluminescence study demonstrated the enhancement and alteration of zinc oxide's optical characteristics. The lithium-doped zinc oxide nanostructure demonstrated exceptional resistance to both Escherichia coli and Staphylococcus aureus germs in the antibacterial testing.

1. Introduction

The research community assuming that the prolonged and continuous use of antibiotics has caused some bacteria to become resistant to them. In order to address this deteriorating situation, it is imperative that new, effective medications be developed as antibacterial agents [1]. Due to their numerous uses, nanotechnology of metal oxide have attracted greater demand in the medical profession. Furthermore, it is well known that metal oxide nanoparticles' large surface area greatly increases their capacity to generate reactive oxygen species (ROS) [2]. Oxidative stress is brought on by the production of ROS. By damaging proteins, cell membranes, and deoxyribonucleic acid (DNA), it causes cellular death [3].Zinc oxide, on the other hand, has outstanding mechanical, electrical, optical, and chemical properties and is a broad band gap semiconductor. Numerous studies have shown that ZnO particles at the nanoscale have potent antibacterial properties against both Gram-positive and Gram-negative bacteria.[4]. Additionally, dopants are added to native ZnO nanocrystals to enhance their antibacterial capabilities [5]. However, lithium was once thought to be a safe metal and was used to treat mental disorders [6].Moreover, with an almost equal ionic radius of lithium (7.6nm) and zinc (7.4nm), incorporation of lithium ions into the ZnO particles has become easy and it affects the physical, and chemical properties directly[7] All these properties enable the ZnO to become effective antibacterial drugs in future.

This task reveals the procedure of synthesis of lithium doped ZnO particles through (Aqueous Chemical Growth) in the presence of low temperature and the evaluation of their ability to fight both type of bacteria whether it is G-Positive or G-negative[8].New bacteria that are resistant to existing antibiotics have emerged as a result of the widespread and excessive usage of antibiotics. The development of novel materials as antibacterial agents is necessary to address this issue [9]. Metal oxide nanomaterials are appealing for use in biomedical applications. It has been suggested that metal oxide nanoparticles' large surface area greatly increases their capacity to generate reactive oxygen species (ROS) [10]. Oxidative stress is brought on by the production of ROS, it can harm proteins, DNA, and cell membranes, which could result in cell death [11].

A wide-band gap semiconductor with superior chemical and physical characteristics is zinc oxide (ZnO). ZnO has been demonstrated to have antibacterial activity against both Gram-positive and Gram-negative bacteria at the nanoscale.[12]. The addition of the appropriate components considerably increased the antibacterial activity [13]. The optical, electrical, and antibacterial properties of ZnO nanoparticles are significantly impacted by the insertion of impurity (Li) in the Zinc oxide, according to previous research [14]. These characteristics make ZnO nanoparticles a potential choice for antibacterial medications. The current study focused on the production of Lithium incorporated Zinc Oxide using a Aqueous Chemical Growth at low temperature and assessed its optical, structural, and antimicrobial characteristics of both type of bacteria G-positive and G-negative [15].

2. Experimental Details Materials

All the chemicals used for the synthesis of Li doped ZnO nanostructures were of analytical grade and used without further processing. Zinc acetate di hydrate Zn(CH3COO)2 2H2O, Lithium Chloride (LiCl), Hexamethylenetetramine (C6H12N4) were purchased from Merck private limited, Karachi, Pakistan. Bacterial cultures were obtained from Liaquat medical Health Science (LUMHS)

Jamshoro, and the Faculty of the Pharmacy University of Sindh Jamshoro.

Synthesis Of ZnO By Aqueous Chemical Method

Li-doped ZnO nanostructures were created by diluting 1.6 grams of zinc acetate di hydrate [Zn(CH3COO)]2H2O in 100 milliliters of deionized water in a 250 milliliter beaker. In a beaker, add 1.05 ml of hexamethylenetetramine (MMT) and dissolve. In the same manner, prepare four beakers of HMT and zinc acetate solution, then add the appropriate amount of lithium chloride (LiCl) to each beaker (5% 0.885 gram, 10% 0.165 gram, and 15% 0.2475 gram), with the exception of one beaker containing pure ZnO. After preparing this solution, vigorously mix it with a magnetic stirrer for ten minutes, or until the water is completely transparent. Finally, all of the beakers were wrapped in aluminum foil and baked for five hours at 95 degrees Celsius in a microwave oven. To reduce the residuals, the final product was lastly filtered using filter paper. Finally, all of the beakers were wrapped in aluminum foil and baked for five hours at 95 degrees Celsius in a microwave oven. In order to minimize residuals, the product was finally filtered through filter paper, cleaned with acetone, and dried overnight at 80 degrees Celsius.

3. Results and Discussion

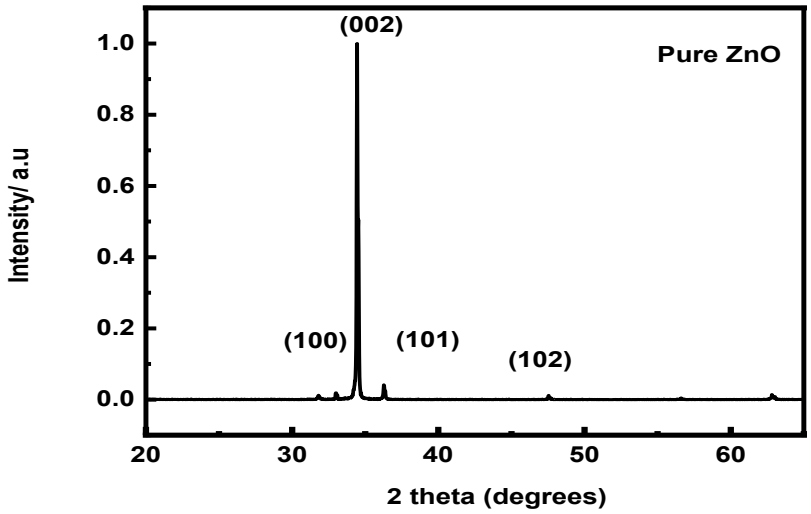

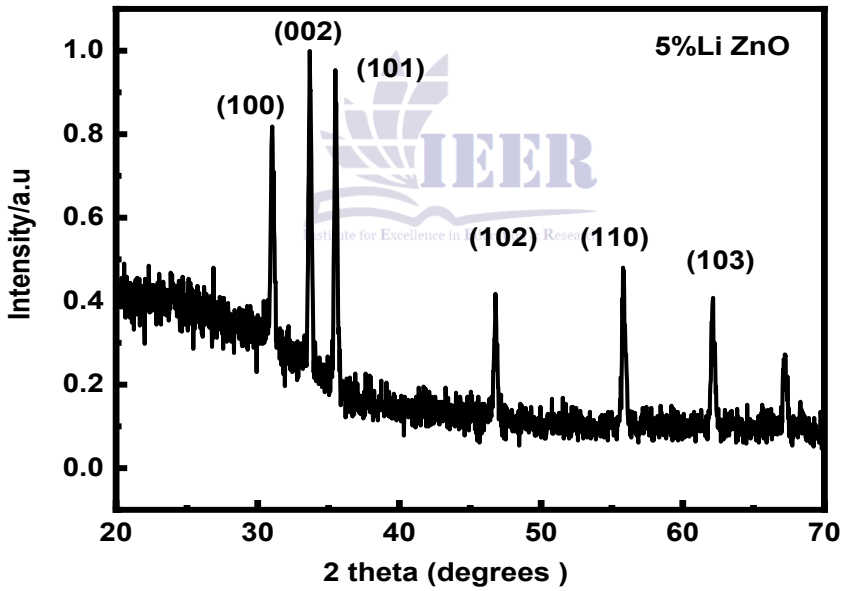

Figure 1(a-b): Shows XRD pattern of sample 1 and 2, which were undoped ZnO and 5% Li doped ZnO

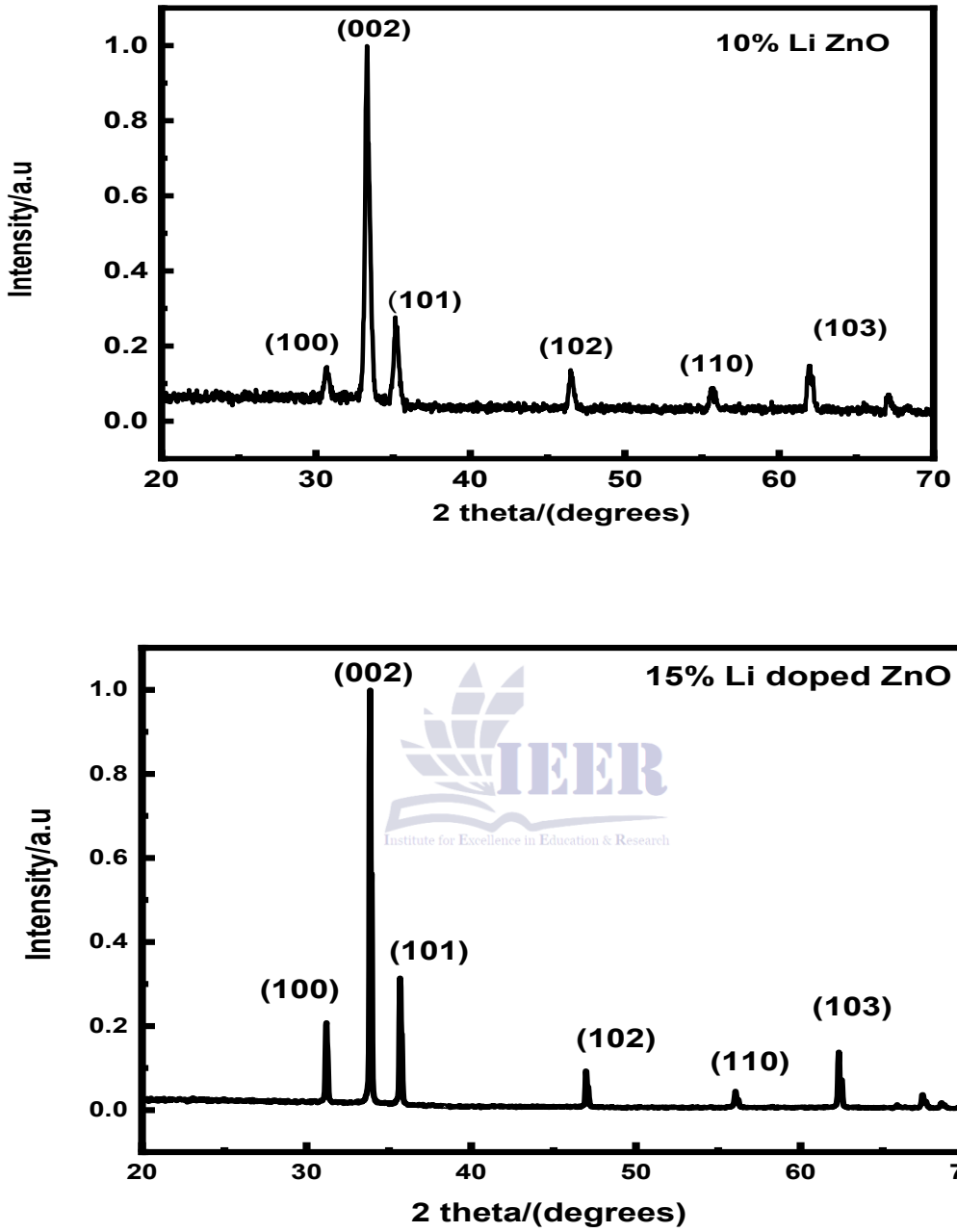

Figure 1(c-d): Shows X Ray Diffraction patterns of sample 3, 4 which were 10% and 15% Li-doped ZnO.

Li-doped ZnO's XRD pattern has been observed between 20 to 80 degrees (2Ø) in figure 1(a-c). All the peaks corresponding to (100), (002), (101), (102), (110), (103) are well indexed with the powder diffraction file (JCPS NO.36-1451), indicating the hexagonal wurtzite phase of ZnO and no other Li related extra peak. This has been revealed that the Li ions have substituted into the Zn lattice site without affecting the crystal structure of ZnO. This because of the same ionic

radius of Lithium ion (7.6nm) being very close to that of Zn ion (7.4nm). Therefore, Li can easily occupy the Zn site in ZnO crystal without any distortion of ZnO crystal.The average crystal size (D) of these samples was measured by utilizing Scherer's formula the Particle Size D = (0.9 x λ)/(d cosθ) λ = 1.54 Å , Θ = 2θ/2, d = full width at half maximum(fwhm) intensity of the peak.

Table 1.1: Represents important parameters of pureZnO and Li doped ZnO nanocrystals

Sample	2θ	d spacing	Fwhm	Hkl	Particle size D
Pure ZnO	34.44	0.2450nm	0.221	(002)	39.33nm
5 % lithium doped ZnO	33.66	0.2664nm	0.3739	(002)	23.19 nm
10%Lithium doped ZnO	33.33	0.2687nm	0.3400	(002)	25.48 nm
15 % lithium doped ZnO	33.80	0.2648nm	0.1244	(002)	69.74 nm

The aforementioned results are according to the (002) reflections' highest value. From pure ZnO to 10% Li doped ZnO, the value of 2θ fell; however, from 5% and 10% Li doping, it slightly increased (34.44 nm at pure ZnO, 33.6 nm at 5% Li doping, 33.3 nm at 10% Li doping, and 33.8 nm at 15% Li doping). From 39.33 nm to 25.6 nm, the particle size shrank.

Nevertheless, fwhm at pure ZnO was lower than that of Li-doped ZnO materials. The computed fwhm trend for doped ZnO shows that the fwhm value initially increased at 5% and 10%.Li doping then declining at 15%. This could be because the ZnO crystal structure contains a higher amount of Li. A trend with Li doping is also seen in the plan separation "d" data. The value of d grew along with the doping. This pattern implies that Li doping is necessary for plan separation.
All of the crystal's surface areas are occupied by more Li ions, which also widen the gaps between planes this was also demonstrated in Particle size measurements, which previously revealed 23.19 nm at 5%, 25.48 nm at 10%, and 69.74 nm at 15%.

Table 1.2: Values of Crystal Strauctur Constant ZnO and Lithum incorporated ZnO

Sample	2theta	Particle size D	Hkl	d spacing	Lattice parameter "a"	Lattice parameter "c"	The ratio of c/a
ZnO	34.44	39.33nm	(002)	0.245nm	0.30nm	0.52 nm	1.73
5% Li doped ZnO	33.66	23.19 nm	(002)	0.266nm	0.30 nm	0.53 nm	1.72
10% Li doped ZnO	33.33	25.48 nm	(002)	0.268nm	0.31nm	0.53nm	1.70
15% Li doped ZnO	33.80	69.74 nm	(002)	0.264nm	0.30nm	0.53 nm	1.73

The formula was used to determine the hexagonal crystal's structure where "a" and "c" were lattice constants.

i. $a = \lambda/\sin\theta$
ii. $c = \lambda/^{1/2}3\sin\theta$

The X-ray's wavelength, "λ," is about equal to 0.1540 nm, and its angle is equal to '2θ'.
Using the above formula, the value of the "d" spacing was determined.

$1/ d^2_{hkl} = 4/3 [h^2 + hk + k^2 / a^2] + l^2/ c^2$

"d" represents the separation between two planes, "a" and "c" represent lattice constants, and "hkl" represents miller indices. The above-calculated results show that pure and Li-doped ZnO have the same crystal structure, with slightly higher c/a ratios to an ideal ratio of 1.633. The value of parameter "a" at hkl (002) was the same for both doped and pure ZnO, except for 10% Li doping. This pattern may indicate that the ZnO unit cell grew in "a" and "b" dimensions at this doping, even though all values were 0.30. It was somewhat larger at 0.31. But at all doping levels, the "c" parameter likewise increased from 0.52 nm at pure ZnO to 0.53 nm. It's possible that lithium filled every space where zinc wasn't present. The literature states that defects, the concentration of external impurities, and the difference in ionic radii to the substitute matrix ion are typically responsible for the lattice constants of semiconductors. This shows that Li^{+1} ions have been added to the crystal lattice, which results in slight structural distortions due to the ionic radius differences between Zn^{+2} (0.74 A °) and Li^{+1} (0.76 A °) ions as well as the formation of O_2 vacancies to counteract the charge instability on the crystal lattice.

Range of the c/a ratio was 1.70 to 1.73. This number is nearly identical to the optimal value for hexagonal crystal cells, c/a ~ 1.63. The interplanar spacing "d" is closely correlated with the value of crystal size. Because the Li atom has the same ionic radius, it can fit into vacant and interstitial sites without altering ZnO's morphology.

SEM Results

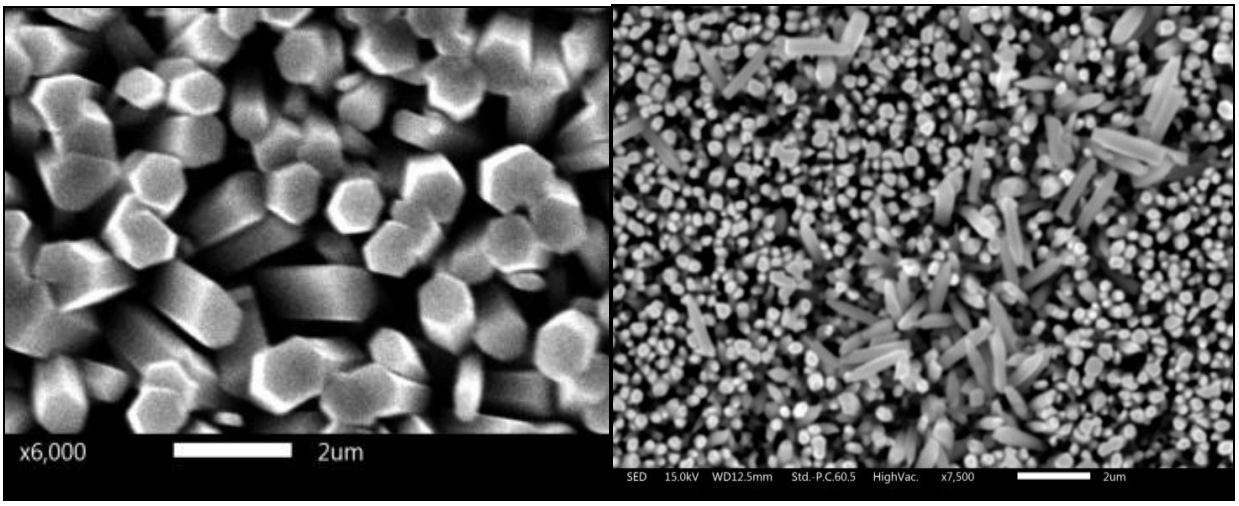

2- a (pure ZnO) 2-b (5% Li ZnO)

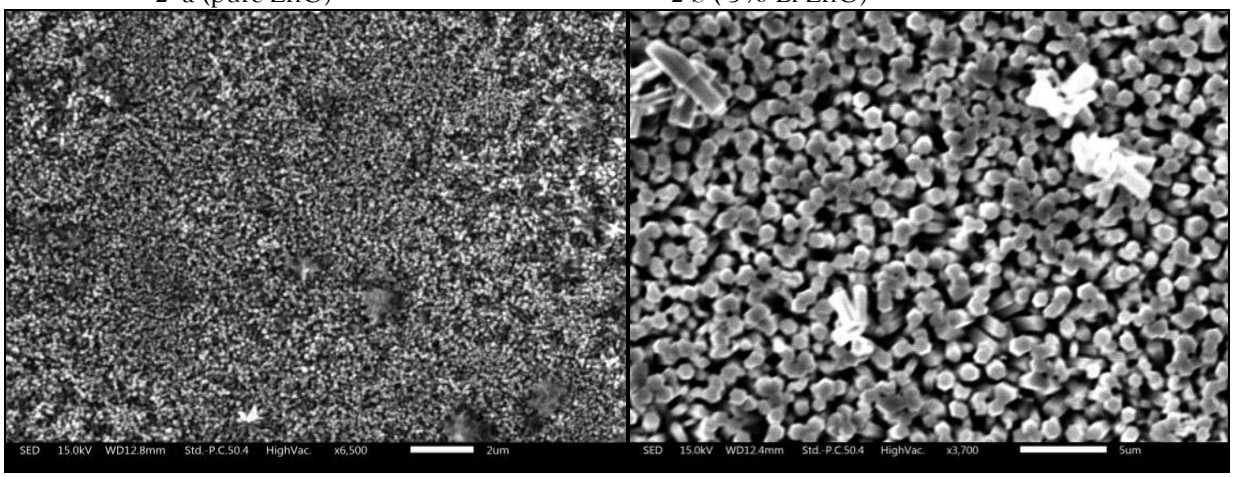

2-c (10% Li ZnO) 2-d (15% Li ZnO)

Figure 2(a–d) displayed SEM pictures of sample-1 undoped ZnO, sample-2 Lithium dpoed-ZnO 5%, sample-3 Lithium doped-ZnO 10%, and sample-4 Lithium doped-ZnO 15%. The hexagonal rod-like shape of pure ZnO nanostructures has been verified by the SEM data. The gown ZnO nanorods are one-dimensional nanostructures with a homogeneous and rod-like shape.

SEM Results of ZnO Doped with 5% Lithium

The results has shown that hexagonal-shaped, rod-like ZnO nanostructures doped with 5% lithium crystal structures. According to the SEM image, there is no change in the crystal shape; all rods exhibit a homogeneous and uniform phase. Additionally, doped ZnO nanorods have the same dimensions too.

SEM Results of ZnO Doped with 10% Lithium

The10% lithium doped ZnO nanostructure was also hexagonal rod-like shape of and identical to that of pure ZnO and 5% Li doped ZnO. According to the SEM image the crystal phase remained unchanged, and all of the crystals had a homogenous and uniform phase.

SEM Results of ZnO Doped with 15% Lithium

The15% Li doped ZnO nanostructures were also hexagonal rod-like shaped, which was identical to that of pure ZnO and doped ZnO at 5% and 10%. This has been validated by a SEM image. The morphology of Li doped 15% ZnO did not change.The undoped and doped forms of ZnO crystals had the same shape and geometry and verified from SEM data.

The overall SEM results indicate that the shape of ZnO nanorods has not been impacted by lithium. This indicates that Li doping gives us the same ZnO shape but with very different physical and chemical characteristics.

Photoluminescence Properties Of Pure & Li Doped Zno

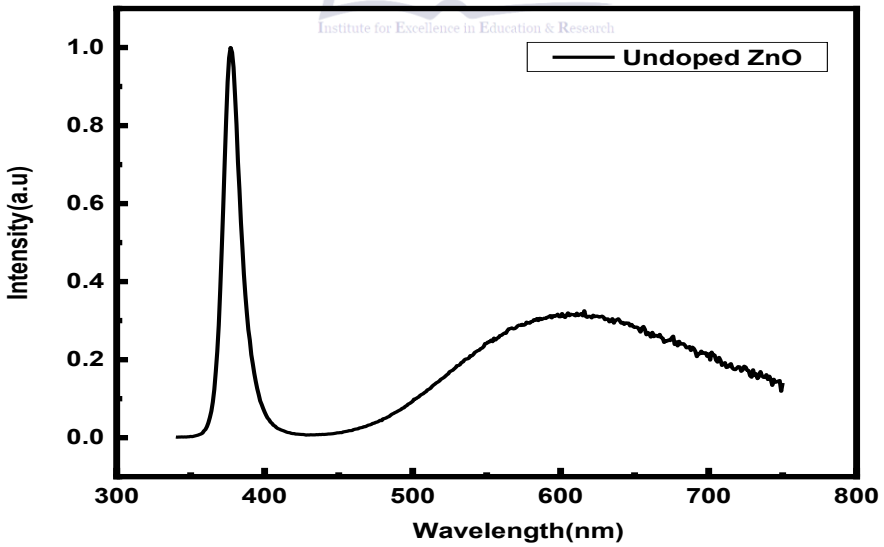

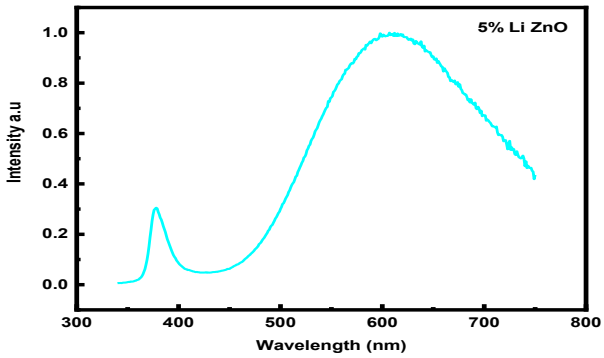

Figure 1(a-b): highlights PL patterns of sample-1& 2, undoped ZnO, & 5% Li-ZnO.

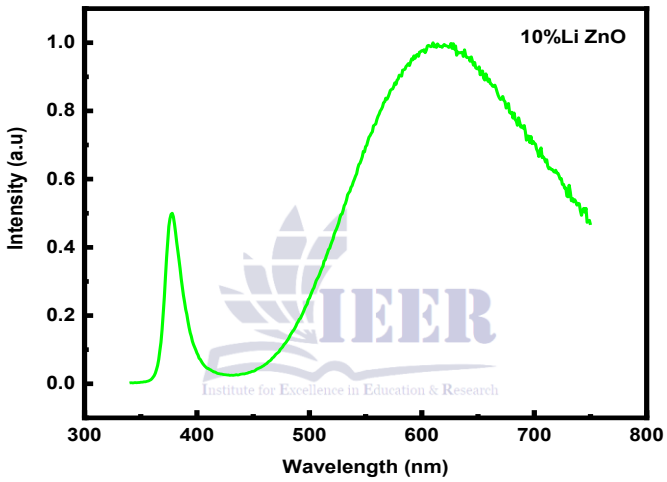

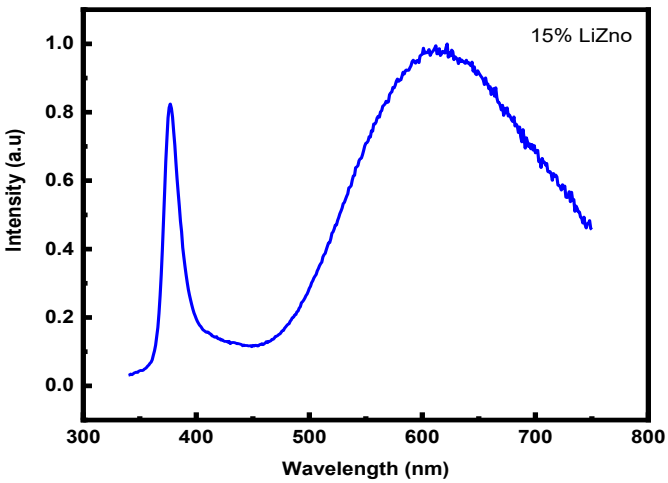

Figure 3(c-d): Shows PL patterns of sample-3& 4, 10% Li- ZnO, and 15% Li-ZnO.

Pure ZnO is an N-type semiconductor, as demonstrated by the photoluminescence graphical pattern (3-a). There are two peaks on the intensity and wavelength graph. The ultraviolet emission peak, also known as the NBE (Near Band Edge) peak. That was the first sharp peak. Nevertheless, the acceptor peak is a larger peak.

Because of ZnO has a larger concentration of holes, 5% Li doped photoluminescence graphical trends (3-b) show that Li-doped ZnO has been turned as a p-type semiconductor due to the Li dopants. The NBE emission peak was smaller, and indicating a drop in electron concentration. Nevertheless, the acceptor (Holes) peak was larger, which indicating that the material contains holes or oxygen vacancies. The acceptor peak's intensity indicated that there was less energy in the radiation that was released, which indicates that the wavelength of the light that was released would be shorter than that of the unhoped ZnO. The band-gap variation might be the cause of this fact.

Regarding 5% Li doped ZnO, the UV emission peak will be greater in the 10% graph (3-c), while the intensity of the visible peak was the same. This pattern implies that the electron concentration has been raised gradually but not as much as that of holes; this could be because of the Li element's amphoteric electrical activity. Because lithium atoms nearly completely replace zinc interstitials and vacancies, the concentration of oxygen vacancies was higher than that of zinc interstitials. This might offer a good chance to recombine visible light-emitting electron and hole exactions.

Compared to the 5% and 10% Li doped ZnO peaks, the U.V. emission peak in the 15% graph was smaller and sharper. This pattern suggested to increase UV emission because of the interstitial zinc and lithium atoms. This could be because the (Zni) and (vo) locations of the crystal were nearly filled with Li atoms. The concentration of wholes or oxygen vacancies was constant since the larger peak remains at the same intensity level. Li's amphoteric nature was causing an increase in Zn interstitials. This indicates that a greater state of Li defect production has been reached. In comparison to earlier doping levels of 5% and 10%, this was the cause of increased UV and visible area emission. Li doping.

Lithium-Doped and Undoped ZnO Photoluminescence Properties

The synthesized material was p-type, as demonstrated by the red-shift in the UV emission peak in Li-doped nanorods. The visible peak graph and UV intensity both demonstrate that peak variation was depended on lithium doping. Lithium doping has changed optical and electrical properties, as the comparative graph has showed it. Doping and lithium concentration have a relative impact on UV emission peaks. A wider visible emission peak, however, remains basically unchanged. After being altered during the first doping phase, it remained at the same intensity.

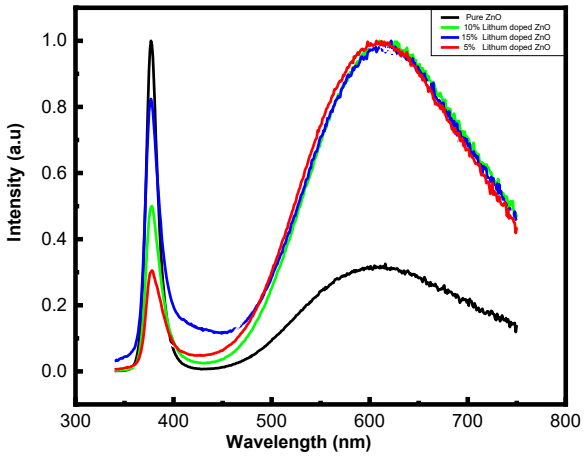

Figure 4: Shows Photoluminescence patterns of Li doped ZnO versus undoped ZnO.

The above results highlighted this fact that zinc interstitials were present in synthesized materials, the comparison graph also verified that pure ZnO is an n-type semiconductor. Furthermore, zinc interstitials and zinc vacancies also emit UV light, whereas oxygen vacancies and oxygen interstitials determine the visible region. However, graphical trends of lithium-doped zinc oxide have demonstrated that the presence of holes or larger oxygen defects caused the material to fully transform into a P-type semiconductor.

Li Doping ZnO's Effects on the Energy Band Gap

The photoluminescence graph was used to compute the bandgap energy. The graphical trend shows that the addition of Li doping at various concentrations causes variations in ZnO's energy gap.

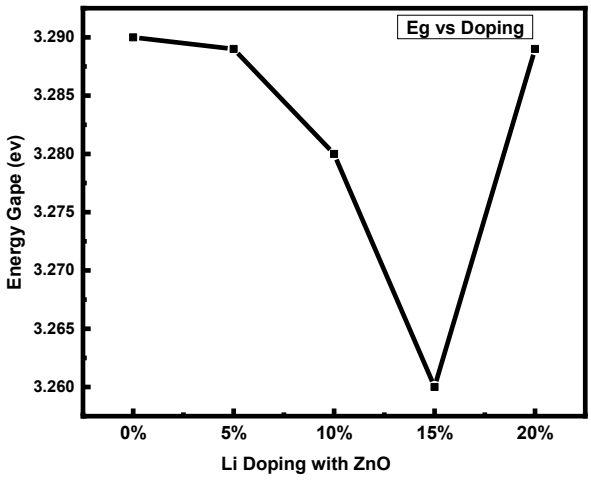

A graph between band gap and Li doping is displayed in Figure 5.

The first three trends, which were 5%, 10%, and 15%, indicated that the band gap value was decreasing and suddenly it rose again and was showing increasing pattern at 20%. At 15%

doping, the Photoluminescence graph's lowest value was 3.260 eV. At 0% doping, however, the value was greater and equal to 3.290. These significant patterns demonstrated that the significant effects of lithium doping had been affected on ZnO's bandgap. Thus, its electrical and optical characteristics have also been altered.

Antibacterial findings of Pure and Li-Doped ZnO Against E. Coli Bacteria

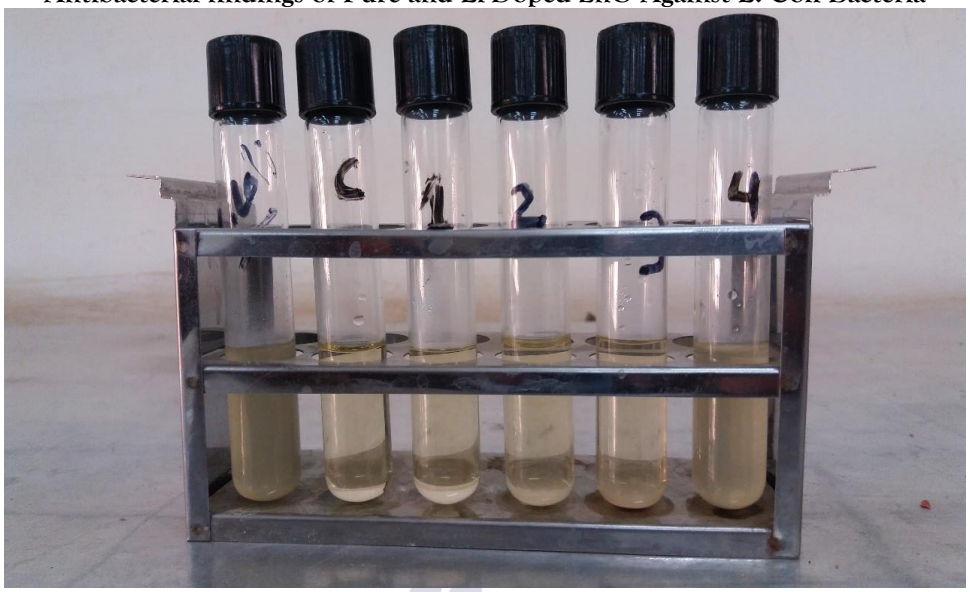

Figure 6 illustrates how reduced the turbidity of solution by using ZnO and Li doped Zno against E.Coli.

Pure and Li-doped ZnO have been tested for their antibacterial properties against Escherichia coli (E. coli) germs. The antimicrobial effects of ZnO and Li doped ZnO nanocrystals were tested using the broth dilution method, which involved pouring 100 milliliters of standardized broth solution into six test tubes, each of which received five milliliters of broth solution. Next, 0.2 milliliters of bacterial culture (E. coli) were combined with five milliliters of each test tube's solution, with the exception of the control test tube. Furthermore, four previously designated pure solutions (5%, 10%, and 15% lithium doped ZnO) and 0.1 milliliters were added to the materials' susceptibility to E. Coli.

Table 1.3: Antibacterial Effect of Li-doped and pure zinc oxide against E. Coli bacteria

Absorbance of control	Absorbance of E.colie	Absorbance of LiZnO & Pure ZnO		Growth Time
0.01	0.075	ZnO	0.047	48 H
0.01	0.075	5%Li ZnO	0.0017	48H
0.01	0.075	10%Li ZnO	0.026	48 H
0.01	0.075	15%Li ZnO	0.034	48 H

Spectroscope results showed that the absorbance of the culture was 0.01 and the absorbance of the E. Coli 5m solution was 0.075. However, the antibacterial activities were altering the Li-doped and pure ZnO absorbance trends. The presence of fewer E. Coli bacterial cells at 5% lithium doped ZnO was indicated by the reduced absorbance at 5% doping. Bacterial growth rose again after this range though not as much as it had in the E. Coli solution. This information

showed that all solutions, whether Li-doped or undoped ZnO, had reduced bacterial turbidity. Every bacterial culture took 48 hours to grow.

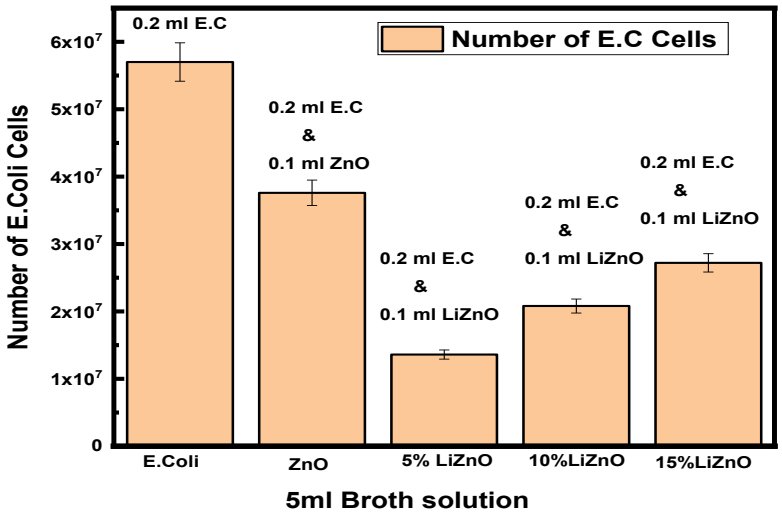

Figure 7: Bar graph of number E.Coli cells in 5ml broth solutions to Zno/LiZnO

Graphical bars demonstrated the effectiveness of ZnO and Li-doped ZnO against E. coli bacteria. At 5%Li doped ZnO, we discovered the smallest bar representation, which corresponds to the fewest cells in 5ml broth solutions. This suggests that when ZnO or LiZnO are absent from the solution, the quantity of E. Coli bacteria is at its highest. However, the highest bar is achieved in a free solution without ZnO or Li-doped ZnO being added.While pure, 10%, and 15% ZnO also show antibacterial tendencies (5% > 10% > 15% > pure ZnO), this sample is used as a reference.

Antibacterial Findings of Pure Zno And Li-Doped Zno Against Staphylococcus Aureus Bacteria.

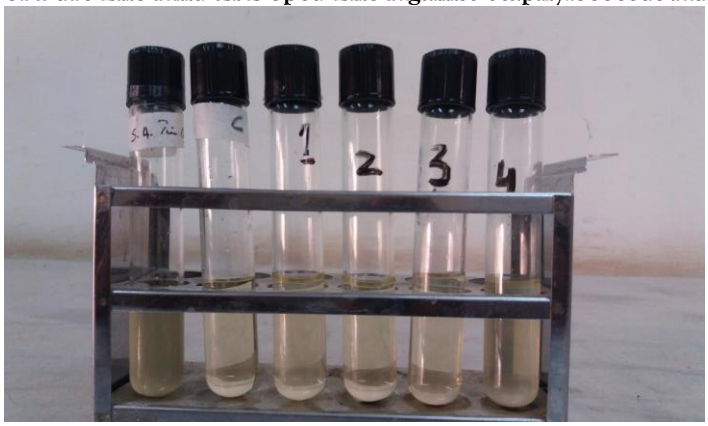

Figure 8 illustrates how the addition of ZnO and Li-doped ZnO against S. aureus bacteria at varying concentrations which were able to reduced the turbidity of the solution.

Using the broth dilution method, the antimicrobial properties of Lithium incorporated Zinc Oxide and pure Zinc Oxide were investigated on S.Aureus germ. This involved pouring 5 milliliters of broth solution into six separate test tubes, adding 0.2 milliliters of bacterial culture to each test tube for contamination purposes, and then adding 0.1 milliliters of ZnO and Li doped ZnO with varying doping concentrations of 5%, 10%, and 15% to each test tube, with the exception of the control test tube. All test tubes were incubated at 370 degrees Celsius for a full day in order to obtain results.

ZnO, 5% LiZnO, 10% LiZnO, and 15% LiZnO were indicated by the test tube marks 1, 2, 3, and 4. The turbidity of the solutions indicated a higher number of bacterial cells, which was linearly correlated with an optical density at a wavelength of 600 nm. The culture solution was the least turbid, whereas the S. aureus solution was the most turbid. For the S. aureus solution, the turbidity of ZnO to Li doped ZnO reduced. The S.Aures test tube with label S.A had the maximum turbidity. This test tubes was also placed 24 hours incubation period against the absence of any ZnO content. After 24 hours, it was shown that the concentration of 5% Li doped ZnO produced the least amount of S. aureus growth; thus, turbidity was also reduced. This figure also shows how different 10% and 15% Li doped ZnO solutions significantly changed the bacterial turbidity.

Table 1.4: Antibacterial results of ZnO and LiZO against Staphylococcus Aureus

Absorbance of control	Absorbance of S.Aureus	Absorbance of LiZnO & Pure ZnO		Growth Time
0.01	0.075	ZnO	0.045	24 Hour
0.01	0.075	5%Li ZnO	0.015	24 Hour
0.01	0.075	10%Li ZnO	0.025	24 Hour
0.01	0.075	15%Li ZnO	0.030	24 Hour

The antibacterial effects against S. aureus at varying Li doping levels (5%, 10%, and 15%), respectively, are displayed in Table 1.4. The S.Aureus-labeled test tube had no antimicrobial material, and the maximum number of S.Aureus cultures indicated the highest turbidity in the broth medium, as indicated by the higher absorbance of 0.075.As we added antimicrobial samples, the absorbance of the remaining test tubes fell. A higher cell inhabitance effect in broth solution was demonstrated by the absorbance of 0.1 ml pure ZnO, 0.2 ml S. aureus, and 5 ml culture, which was 0.045. Additionally, Li-doped ZnO demonstrated significant impacts on S. aureus culture; 5% Li-doped ZnO produced the lowest antibacterial outcomes. The absorbance of ZnO was 0.015, indicating the lowest number of cells in solution; the absorbance at 10% and 15% was 0.025 and 0.030, respectively, with a 0.005 absorbance difference. This finding demonstrated that various Li doping in ZnO could have antibacterial effects against S. aureus but the prominent effects were found when the the least amount of Li doped ZnO present in solution this might be caused due to the smaller size of crystal enhance the ROS mechanism and ultimate cause of death of S.Aurus bacteria.

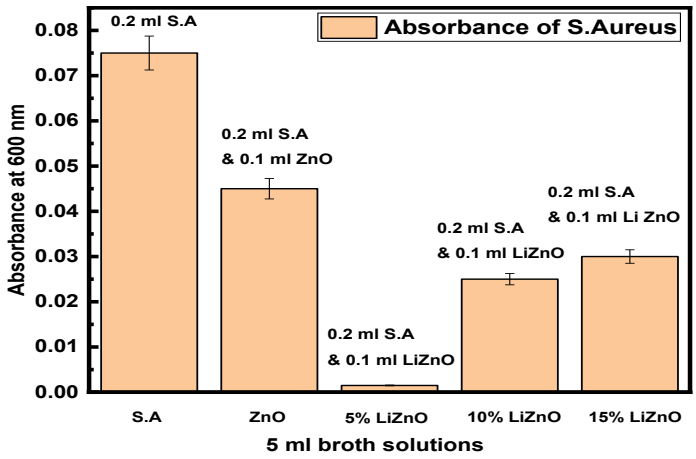

Figure 9: Absorbance vs 5 ml broth solutions with varying ratios of ZnO/Li doped ZnO and S. aureus bacteria

In the figure.9 of bar graph has shown that solution was free from ZnO and Li doped ZnO antibacterial substance dosages the S.Aureus bacterial growth was predominated. The S.Aureus solution's light absorbance at 600 nm was 0.075, indicating a higher turbidity of the medium and more bacterial cells in the solution. The remaining sample findings, demonstrated strong antibacterial properties ranging from Li-doped ZnO at 5%, 10%, and 15% to pure ZnO. In comparison to all samples, the 5% Li doped ZnO solution exhibited the lowest absorbance and the highest transparency, indicating that it had more potent antibacterial qualities. This effects may be observed due to the particle size of 23 nm on S. aureus.As a result, 5% Li doping in ZnO may have the greatest harmful effects against S. aureus bacteria this was only possible when a variety of processes, including the release of highly reactive ions and the production of hydrogen peroxide, the more toxic effects restricted bacterial growth and reduced the quantity of germs from the medium. Therefore, the findings above show that at 5%, 10%, and 15% Li doped ZnO, more ROS and H_2O_2 were generated.

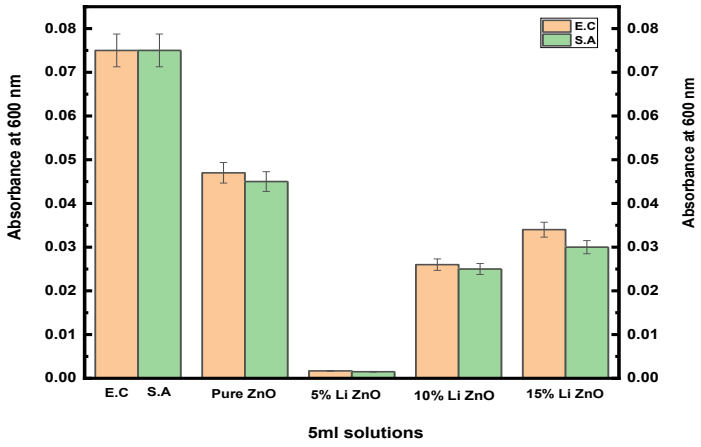

Figure 10: Absorbance vs 5 ml broth solutions with varying concentrations of ZnO/Li doped ZnO, E. Coli, and S. aureus.

A comparison bar graph of two gram-positive and gram-negative bacterial species, E. Coli and S. Aureus, is displayed in Figure 10 in relation to the absorbance of a 5 ml broth solution at a wavelength of 600 nm. Both bacterial species had developed exponentially in the 5 ml broth medium, according to the bar graph, and they were displaying a higher absorbance value of 0.075. The inclusion of 0.1 ml of pure ZnO in solution significantly reduced the absorbance of the same bacterial species by 0.045 at S. aureus and 0.047 at E. coli in the ensuing bar comparison. A slight variation in the S.Aureus bar has also been observed; this variation was linked to pure ZnO nanoparticles, which were more deadly to S.Aureus than E. coli. Because Li-doped ZnO was more dangerous and had a small particle size of 23.19 nm, the subsequent graphical bars at 5% of two species were completely suppressed. At E. Coli and S. Aureus, the measured light absorbance was 0.017 and 0.015, respectively indicating a decreased absorbance of light in solution. The least amount of bacteria in both solutions was indicated by the lowest absorbance. In comparison to 5% and pure ZnO, the 10% Li doped bar trends of both bacterial species remained greater. The S. Aureus bar also showed a minor shift that was less pronounced than the E. coli trend. This might be the result of various bacterial species exhibited distinct harmful effects against Li ZnO doped. Different absorbencies at the same Li doping were displayed in the final two bar graphs of E. Colie and S. Aureus. E. Coli and S. aureus had absorbance values of 0.034 and 0.030, respectively. Gram-positive bacteria S. aureus were more sensitive to Li-doped ZnO nanoparticles than Gram-negative bacteria E. coli, as indicated by the small absorbance difference of 0.004.

4. CONCLUSION

In this study, we used a low temperature (ACG) method to create Li-doped ZnO nanoparticles (NPS). And performed characterization of X-ray diffraction (XRD), scanning electron microscopy (SEM), UV-Vis spectroscopy, and photoluminescence (PL) to analyze the low-temperature produced Li Doped ZnO nanoparticles in order to determine their fundamental and optical characteristics. Besides this the antibacterial effects on both gram-positive and gram-negative pathogens was also targeted by the using broth dilution method, the targeted species were S. aureus E. coli. The XRD analysis verified that the produced doped nanostructures are hexagonal and wurtzite. SEM analysis revealed that every nanostructure produced is homogenous and resembles a 1D rod. The photoluminescence analysis validated that ZnO's optical characteristics have been altered and enhanced. It also demonstrated that the integration of Li in varying percentages has reduced ZnO's band gap. Li ZnO nanostructures demonstrated exceptional resistance to the targeted microorganisms in the antibacterial research.

5. Ethical Compliance

This research experiments conducted in this article with two bacterial species that were approved by the responsible authorities of the University of Sindh, Institute Of Biotechnology, following all guidelines, regulations, legal, and ethical standards as required for antimicrobial testing.

6. Conflicts of Interest

No any conflict of interest.

7. Acknowledgments

I acknowledge to this paper to my loved one for helping me to complete this assignment and publish it for the benefit of humanity.

5. REFERENCES:

[1] Fair, R.J. and Tor, Y., 2014. Antibiotics and bacterial resistance in the 21st century. *Perspectives in medicinal chemistry*, 6, pp.PMC-S14459.

[2] Naseem, T. and Durrani, T., 2021. The role of some important metal oxide nanoparticles for wastewater and antibacterial applications: A review. *Environmental Chemistry and Ecotoxicology*.

[3] Sharma, P., Jha, A.B., Dubey, R.S. and Pessarakli, M., 2012. Reactive oxygen species, oxidative damage, and antioxidative defense mechanism in plants under stressful conditions. *Journal of botany*, *2012*.

[4] Siddiqi, K.S., ur Rahman, A. and Husen, A., 2018. Properties of zinc oxide nanoparticles and their activity against microbes. *Nanoscale research letters*, *13*(1), pp.1-13.

[5] Sadaiyandi, K., Kennedy, A., Sagadevan, S., Chowdhury, Z.Z., Johan, M.R.B., Aziz, F.A., Rafique, R.F. and Selvi, R.T., 2018. Influence of Mg doping on ZnO nanoparticles for enhanced photocatalytic evaluation and antibacterial analysis. *Nanoscale research letters*, *13*(1), pp.1-13.

[6] Shorter, E., 2009. The history of lithium therapy. *Bipolar disorders*, *11*, pp.4-9.

[7] Oquendo-Cruz, A. and Perales-Pérez, O., 2018. Synthesis, characterization and bactericide properties of pure and Li doped ZnO nanoparticles for alternative water disinfection methods. *Journal of Electronic Materials*, *47*(10), pp.6260-6265.

[8] Sirelkhatim, A., Mahmud, S., Seeni, A., Kaus, N.H.M., Ann, L.C., Bakhori, S.K.M., Hasan, H. and Mohamad, D., 2015. Review on zinc oxide nanoparticles: antibacterial activity and toxicity mechanism. *Nano-micro letters*, *7*(3), pp.219-242.

[9] Ventola, C.L., 2015. The antibiotic resistance crisis: part 1: causes and threats. *Pharmacy and therapeutics*, *40*(4), p.277.

[10] Nikolova, P.Maria, M.SChavali., 2020. "Metal Oxide Nanoparticles as Biomedical Materials." Biomimetics (Basel, Switzerland), vol. **5** (2), p. 27.

[11] Sharma, P., Jha, A.B., Dubey, R.S. and Pessarakli, M., 2012. Reactive oxygen species, oxidative damage, and antioxidative defense mechanism in plants under stressful conditions. *Journal of botany*, *2012*.

[12] Gudkov Sergey V., Burmistrov Dmitriy E., Serov Dmitriy A., Rebezov Maxim B., Semenova Anastasia A., Lisitsyn Andrey B.

[13] Gudkov, S.V., Burmistrov, D.E., Serov, D.A., Rebezov, M.B., Semenova, A.A. and Lisitsyn, A.B., 2021. A Mini Review of Antibacterial properties of ZnO nanoparticles. *Front. Phys. 9: 641481. doi: 10.3389/fphy*.

[14] Wang, L., Hu, C. and Shao, L., 2017. The antimicrobial activity of nanoparticles: present situation and prospects for the future. *International journal of nanomedicine*, *12*, p.1227.

[15] Rakkesh, R.A. and Balakumar, S., 2014. Structural, electrical transport and optical studies of Li ion doped ZnO nanostructures. *Processing and Application of ceramics*, *8*(1), pp.7-13.